

# Evaluation of Usability on Mobile Detector X-ray Absorption, Scattering, and Phased Image Phantom

Chang-Gyu Kim

*Department of Radiological Science, Gimcheon University*

## ABSTRACT

Existing X-ray medical imaging acquired the image data of X-ray absorption difference using the difference in density of the subject tissue. X-ray scattering and phase contrast imaging technology is a technology that dramatically increases boundary information between homogeneous materials of similar density using scattering and phase contrast information. To acquire and evaluate absorption, scattering, and phase contrast images, using the phantom made of polyethylene, on a round rod with a diameter of 3×1cm, a hole with a diameter of 0.5cm was drilled on 5 round rods, and the medical phantom was produced by sealing with sodium chloride, neon, calcium, phosphorus, and selenium powder. At a distance of 40cm from the focus, the distribution of absorbed doses have shown  $1,277 \pm 0.31\mu\text{Gy}$  in the center area. The measurement dose in the anode side direction was  $110.1 \pm 0.35\mu\text{Gy}$  and the cathode side direction was  $117.7 \pm 0.77\mu\text{Gy}$ . It has shown dose inequality that depends on the geometry of the target. It has shown similar tendency in 60cm and 80cm Compared with absorption images in graphite materials, it was confirmed that scattering and phase contrast images were showing relatively high image information. These results are expected to be utilized as an important basic data for reducing medical exposure dose and acquiring, evaluating and utilizing X-ray absorption, scattering and phase contrast images.

**Keywords:** *Absorption, Scattering, Phase contrast, Usability, Radiation healthcare*

## Introduction

The X-ray was discovered on Friday evening, November 8, 1895 by Professor Röntgen. It has great historical significance to science such that it was deemed to have opened the age of modern physics. X-ray is generated by colliding accelerated electrons under high voltage against a metal plate called a target using a kind of vacuum discharge tube called an X-ray tube. For the types of X-rays, there is braking radiation that generates electromagnetic waves while suddenly stopping due to the Coulomb force when accelerated electrons pass near nuclei of tungsten objects, and if the electrons of the K angle are empty, there is a characteristic X-ray which is generated as the electron of L angle transits. The probability of X-ray occurrence is 90% for braking radiation, and 10% for characteristic X-ray<sup>[1-5]</sup>.

X-ray wavelength is shorter than ultraviolet ray and longer than gamma ray. X-rays and gamma rays have a short wavelength and high energy, so they penetrate deep inside the matter. Because of this nature, with X-rays, we can look into the inside of a material like magic. Because X-rays are not directly visible, it is necessary to convert the image to a visible image using a film or a detector. The x-ray detector is made using the properties of X-ray ionizing the matter. Here, ionization means a phenomenon in which atoms and electrons are separated into positive ion and free electron by releasing electrons from neutral atoms.

The most important applications of X-ray are medical diagnosis. The X-ray was the only way to obtain images of the inside of a human body without damaging the human body until the introduction of ultrasound in 1953 or magnetic resonance imaging technology in 1973. But with the emerging of electronics and a rapid development of computers, X-rays are used not only for simple imaging but also for various methods such as computed tomography(CT, 1970s ~), fluoroscopy (1950's~), and digital tomosynthesis, etc.

---

### Corresponding Author:

Chang-Gyu Kim

Department of Radiological Science,  
Gimcheon University

Email: radkcg@hanmail.net

Simple imaging is the simplest test of shooting the part of human body such as chest, abdomen, skeleton using x-ray and x-ray films. This test is used to diagnose tuberculosis, pneumonia, lung cancer, kidney stones, and fractures. However, X-ray film has a disadvantage in that it requires the use of toxic substances during development and takes a long time to develop. To complement this, since the 1990s, the digital radiography has been developed to display images on computer monitors immediately after shooting based on amorphous silicon, and currently, various computer aided diagnostics techniques are being used.

Over the past 100 years, advances in various technologies have been made centering on x-ray generator and x-ray detection technology, and it is expanding its use to medical, industrial, food, as well as pure science and arts fields. The application field and scope of X-ray will increase more and more. Since medical radiation using X-rays occupies most of the annual average dose, there are efforts to institutionalize the management of exposure doses, to minimize exposure dose, and to obtain optimal images<sup>[6-9]</sup>.

Existing X-ray medical imaging has acquired the image data of X-ray absorption difference using the difference in density of the subject tissue. X-ray scattering and phase contrast imaging technology is a technology that dramatically increases boundary information between homogeneous material of similar density using scattering and phase contrast information in radiation healthcare[10-15]. In addition, it has a feature of acquiring image with excellent image quality with low radiation dose than existing image acquisition technology using X-ray absorption difference [15-20]. For this reason, in this study, by self producing the phantom that can acquire and evaluate X-ray absorption images, phase contrast images and scatter images, a mobile detector-based absorption doses were evaluated, and X-ray absorption difference images, scattering images, and phase contrast images were obtained with its usability analyzed.

### Research Method

**X-ray Dose Measurement Evaluation:** For the detector the mobile detector of DR Tech was used, and for X-ray generator, the foreign medical equipment CXD-R185 system was used. For dose measurement, the measurement distance of X-ray tube and dosimeter was

40 cm, 60 cm, and 80 cm. For exposure conditions, the average value was obtained by measuring 10 times for each distance condition using the irradiation of 22kVp 20mA 630ms.

For dosimetry device, using a glass dosimeter Dose Ace (Model GD-352M and FGD-1000, Asahi Techno Glass Cooperation, Shizuoka, Japan), the annealing process was heated at 400°C for 1 hour before the dose measurement and the background values were measured after cooling. After measuring the dose under each condition and after the pre-heating is carried out at 70°C for 1 hour, the average value was calculated by repeatedly measuring the integral dose value 10 times through the reader after cooling. Calibration of glass dosimeter used <sup>137</sup>Cs radioactive standard from the Japanese radiation standards to conduct calibration with glass element with 6 mGy irradiated to measure[Figure 1, Figure 2].



**Figure 1: Glass dosimeter measuring element**



**Figure 2: Glass dosimeter device reader and a preheating device**

**Absorption, scattering, phase contrast image acquisition phantom production and image evaluation:** To acquire and evaluate absorption, scattering, and phase contrast images, using the phantom made of polyethylene, on a round rod with a diameter of 3×1cm, a hole with a diameter of 0.5cm was drilled on 5 round rods, and the medical phantom was produced by sealing with sodium chloride, neon, calcium, phosphorus, and selenium powder. Acquisition of absorption, scattering, and phase contrast images were acquired and

analyzed by irradiating it at the exposure conditions of 22kVp 20mA 630msec using a self produced phantom by setting the distance between the focus and subject at 300mm, fixed grid at 700mm, and the distance between the focus and detector at 1,448mm.



**Figure 3: Absorption, scattering, and phase contrast image acquisition radiation healthcare phantom**

### Research Results and Considerations

**X-ray Dose Measurement Evaluation Result:** Using the CXD-R185 X-ray generator, X-ray absorption dose was measured and evaluated with a glass dosimeter by changing the distance of the x-ray focus to 40cm, 60cm, and 80cm. For X-ray irradiation conditions, by setting the irradiation at 22kVp 20mA 630ms, the mean and standard deviation values were measured by measuring 10 times for each condition.

At a distance of 40cm from the focus, the distribution of absorbed doses have shown  $1,277 \pm 0.31\mu\text{Gy}$  in

the center area. The measurement dose in the anode side direction was  $110.1 \pm 0.35\mu\text{Gy}$  and the cathode side direction was  $117.7 \pm 0.77\mu\text{Gy}$ . It has shown dose inequality that depends on the geometry of the target. In addition, with the measurement dose of  $93.3 \pm 0.41\mu\text{Gy}$  in the upward direction and  $60.3 \pm 0.34\mu\text{Gy}$  in the downward direction of focus, the absorbed dose showed a different dose distribution with respect to the focal point.

At a distance of 60cm from the focus, the distribution of absorbed doses have shown  $500.3 \pm 0.16\mu\text{Gy}$  in the center area. The measurement dose in the anode side direction was  $83.5 \pm 0.32\mu\text{Gy}$  and the cathode side direction was  $87.3 \pm 0.31\mu\text{Gy}$ . It has shown dose inequality that depends on the geometry of the target. In addition, with the measurement dose of  $79.2 \pm 0.30\mu\text{Gy}$  in the upward direction and  $47.3 \pm 0.28\mu\text{Gy}$  in the downward direction of focus, the absorbed dose showed a different dose distribution with respect to the focal point.

At a distance of 80cm from the focus, the distribution of absorbed doses have shown  $129.8 \pm 0.31\mu\text{Gy}$  in the center area. The measurement dose in the anode side direction was  $57.0 \pm 0.27\mu\text{Gy}$  and the cathode side direction was  $60.9 \pm 0.16\mu\text{Gy}$ . It has shown dose inequality that depends on the geometry of the target. In addition, with the measurement dose of  $51.2 \pm 0.34\mu\text{Gy}$  in the upward direction and  $37.2 \pm 0.47\mu\text{Gy}$  in the downward direction of focus, the absorbed dose showed a different dose distribution with respect to the focal point[Table 1].

**Table 1: X-ray dose measurement evaluation result**

Direction	Exposure dose (40cm)	Exposure dose (60cm)	Exposure dose (80cm)
Cathode	$117.7 \pm 0.77\mu\text{Gy}$	$87.3 \pm 0.31\mu\text{Gy}$	$60.9 \pm 0.16\mu\text{Gy}$
Anode	$110.1 \pm 0.35\mu\text{Gy}$	$83.5 \pm 0.32\mu\text{Gy}$	$57.0 \pm 0.27 \mu\text{Gy}$
Center	$1,277 \pm 0.31\mu\text{Gy}$	$500.3 \pm 0.16 \mu\text{Gy}$	$129.8 \pm 0.31 \mu\text{Gy}$
Up	$93.3 \pm 0.41 \mu\text{Gy}$	$79.2 \pm 0.30\mu\text{Gy}$	$51.2 \pm 0.34 \mu\text{Gy}$
Down	$60.3 \pm 0.34 \mu\text{Gy}$	$47.3 \pm 0.28 \mu\text{Gy}$	$37.2 \pm 0.47 \mu\text{Gy}$

These results are similar to those of other studies[11-15] and it was confirmed that the dose inequality phenomenon occurs with the same tendency due to the geometrical structure of the x-ray tube in the medical X-ray low energy region. In addition, it was confirmed that as the distance got farther away from the focus, the absorption dose was lowered. This phenomenon shows that when performing a disease

examination using X-ray, it is helpful to keep a far distance as possible.

**Absorption, scattering, phase contrast acquisition, phantom production and image acquisition evaluation result:** To acquire and evaluate absorption, scattering, and phase contrast images, using the phantom made of polyethylene, on a round rod with a diameter of 3\*1cm,

a hole with a diameter of 0.5cm was drilled on 5 round rods, and the medical phantom was produced by sealing with sodium chloride, neon, calcium, phosphorus, and selenium powder. Acquisition of absorption, scattering, and phase contrast images were acquired and analyzed by irradiating it at the exposure conditions of 22kVp 20mA 630msec using a self produced phantom by setting the distance between the focus and subject at 300mm, fixed grid at 700mm, and the distance between the focus and detector at 1,448mm.

**15P material absorption, scattering, phase contrast imaging result**

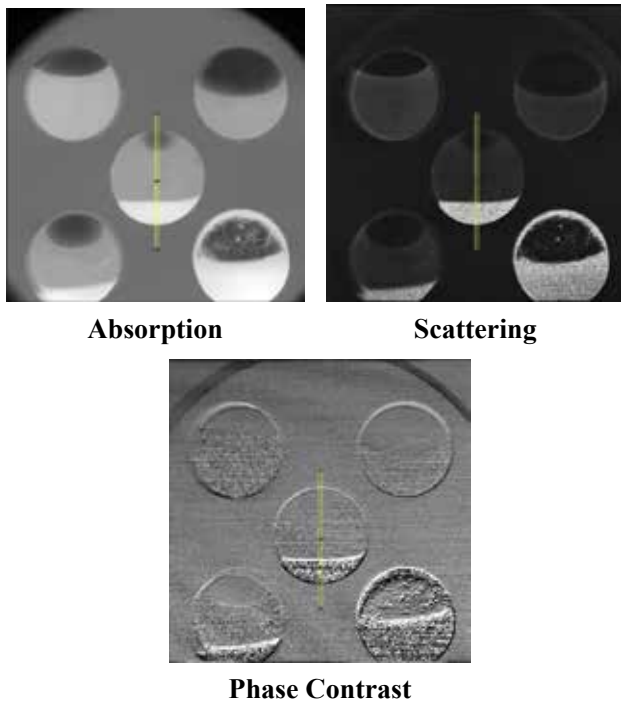


**Figure 4: 15 P material absorption, scattering, phase difference image evaluation result**

X-ray absorption images are obtained by the difference of absorption decay coefficient of the matter, where the larger the density difference of the tissue, the greater the difference in the contrast of the images, it becomes easier to diagnose the disease or to check for foreign matter. On the other hand, X-ray scattering and phase contrast images are obtained by imaging the x-ray velocity difference at two nearby points as the x-ray passes through the matter, thus it is more efficient than X-ray absorption difference image and can reduce radiation dose since the real part of the refractive index that determines this speed is about one thousand times larger than the absorption coefficient in radiation healthcare<sup>[15,19,20]</sup>.

As a result of evaluating the 15P material absorption, scattering, and phase contrast images, the evaluation results of absorption image information and the evaluation results of scattered image and phase contrast image did not show significant difference[Figure 4].

**Nacl material absorption, scattering, phase contrast image result**

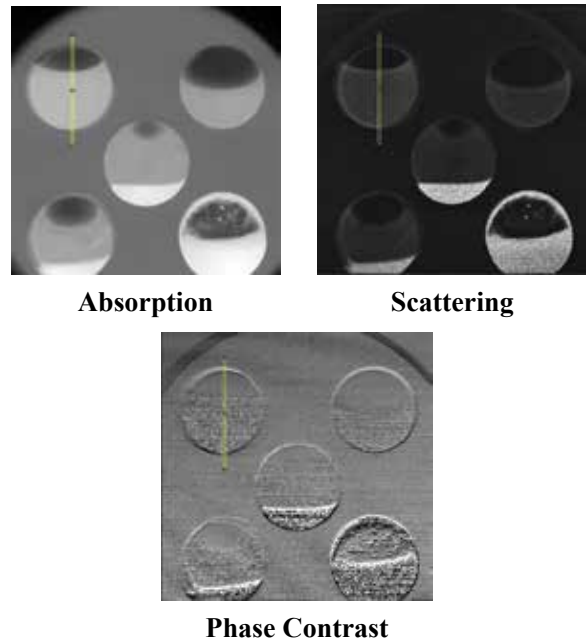


**Figure 5: Nacl material absorption, scattering, phase contrast image evaluation result**

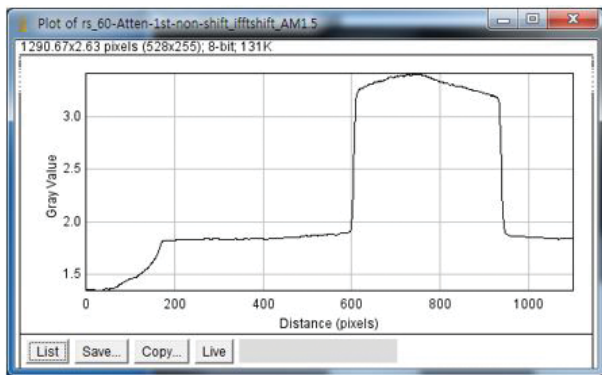
Since the x-ray absorption contrast image is generated by the x-ray attenuation coefficient of the tissue, the distortion of image information occurs according to the geometric location. Overcoming these drawbacks is scattering and phase contrast image. Scattered image and phase contrast provides high discrimination in identifying matters by calibrating the geometric distortion and the degree of scattering through mathematical algorithms.

As a result of evaluating the Nacl material absorption, scattering, and phase contrast images, the evaluation results of absorption image information and the results of scattering and phase contrast images did not show a significant difference[Figure 5].

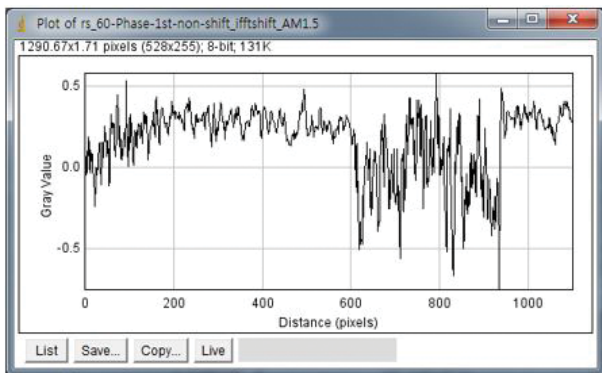
**Graphite material absorption, scattering, phase contrast image result:** Organ or tissue composed of a substance with a low effective atomic number significantly reduces the contrast or resolution of the image in the absorption difference image, therefore the identification ability of the image is deteriorated. However, scattering

and phase contrast images improve the contrast and resolution of images even with low atomic numbers thus it can be helpful for diagnosing diseases from images by increasing the ability to identify images.

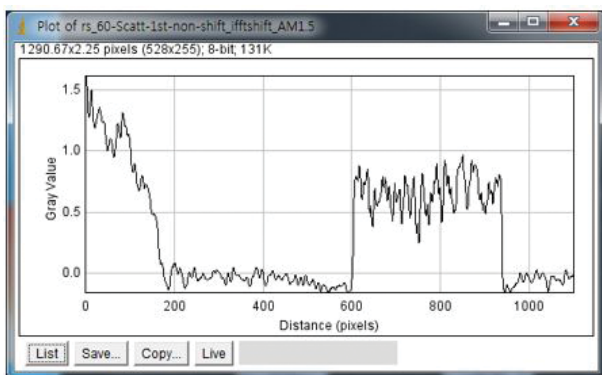
The result of [Figure 6] shows the ability to identify scattered and phase-contrast images when the graphite material with low atomic number is compared with absorption image. It can be seen that although absorption imaging degrades the identification ability, but the identification ability is increased in scattered image and phase contrast images.



**Absorption**



**Scattering**



**phase Contrast**

**Figure 6: Graphite material absorption, scattering, phase contrast image evaluation result**

This result confirms the usefulness of scattering and phase contrast images when describing areas of soft tissue having a low X-ray absorption difference in organs and tissues of the human body. In addition, scattering and phase contrast imaging is a technology that dramatically increases boundary information between homogeneous materials or similar materials with little difference in density, it can be used for clinical breast cancer imaging or low dose computed tomography in radiation health care.

Along with the development of X-ray scattering image and phase contrast imaging technology, it is thought that many studies on the reduction of exposure dose should be carried out with more research and development on medical phantom that can acquire and evaluate images quantitatively.

**Conclusion**

In this study, a phantom that can acquire and evaluate the X-ray absorption, scattering, and phase contrast images was self produced and the X-ray dose was measured, analyzed and its images were obtained and analyzed.

At a distance of 40cm from the focus, the distribution of absorbed doses have shown  $1,277 \pm 0.31\mu\text{Gy}$  in the center area. The measurement dose in the anode side direction was  $110.1 \pm 0.35\mu\text{Gy}$  and the cathode side direction was  $117.7 \pm 0.77\mu\text{Gy}$ . It has shown dose inequality that depends on the geometry of the target. It has shown similar tendency in 60cm and 80cm.

As a result of acquiring and analyzing the absorption, scattering, and phase contrast images of sodium chloride, phosphorus, and graphite materials, there was no difference in the amount of absorption, scattering, and phase contrast images of sodium chloride and phosphorus. Compared with absorption images in graphite materials, it was confirmed that scattering and phase contrast images were showing relatively high image information in radiation healthcare.

These results are expected to be utilized as an important basic data for reducing medical exposure dose and acquiring, evaluating and utilizing X-ray absorption, scattering and phase contrast images.

**Ethical Clearance:** Not required

**Source of Funding:** This research was supported by a Gimcheon University research grants in 2018.

**Conflict of Interest:** The authors declare no conflict of interest.

## REFERENCES

1. Chang-Gyu Kim. "Exposure dose reduction during lateral spine test with water filter". *Technology and Health Care*, (2016).
2. Chang-Gyu Kim, Sun-Youl Seo. A Study on Reducing Exposure Dose of Radiographer Assistants during CT Scan of Injury Patients without Spontaneous Breath. *Jour of Adv Research in Dynamical & Control Systems.*, (2017).
3. Soonmu Kwon, Jungsu Kim. The Evaluation of Eye Dose and Image Quality According to The NewTube Current Modulation and Shielding Techniques in Brain CT. *Journal of the Korean Society of Radiology.*, (2015).
4. Youl-Hun Seoung. Evaluation of Surface Radiation Dose Reduction and Radiograph Artifact Images in Computed Tomography on the Radiation Convergence Shield by Using Sea-Shell. *Journal of the Korea Convergence Society.*, (2017).
5. J. K. Park, I. H. Choi, H. H. Park, S. W. Yang, K. T. Kim, S. S. Kang. "Design of Double Layer Shielding Structure using eco-friendly Shielding Materials". *J.Korean Soc. Radiol.*, (2016).
6. A.W. Stevenson, T.E. Gureyev, D. Paganin, S.W. Wilkins, T. Weitkamp, A. Snigirev. Phase-contrast X-ray imaging with synchrotron radiation for materials science applications. *Nuclear Instruments and Methods in Physics Research.*, (2003).
7. P. Cloetens, M. Pateyron-Salome, J. Y. Buffiere, G. Peix, J. Baruchel, F. Peyrin, and M. Schlenker. Observation of microstructure and damage in materials by phase sensitive radiography and tomography. *J. Appl. Phys.*, (1997).
8. F. Pfeiffer, O. Bunk, C Davidl, M Bech, G. Le Duc, A. Bravin, and P Cloetens. High-resolution brain tumor visualization using three-dimensional x-ray phase contrast tomography. *Physics in Medicine and Biology*, (2007).
9. David C, Bruder J, Rohbeck T, Grunzweig C, Kottler C, Diaz A, Bunk O and Pfeiffer F.. Fabrication of diffraction gratings for hard x-ray phase contrast imaging. *Microelectron. Eng.*, (2007).
10. Pfeiffer F, Kottler C, Bunk O and David C. Tomographic reconstruction of three-dimensional objects from hard x-ray differential phase contrast projection images. *Nucl. Instrum. Meth. Phys.*, (2007).
11. FRANZ PFEIFFER, TIMM WEITKAMP, OLIVER BUNK AND CHRISTIAN DAVID. Phase retrieval and differential phase-contrast imaging with low-brilliance X-ray sources. *Nature Physics.*, (2006).
12. Pagot, E. et al. Quantitative comparison between two phase contrast techniques: diffraction enhanced imaging and phase propagation imaging. *Phys. Med. Biol.*, (2005).
13. Anna Burvall, Ulf Lundstrom, Per A. C. Takman, Daniel H. Larsson, and Hans M. Hertz. Phase retrieval in X-ray phase-contrast maging suitable for tomography. *Optical Society of America.*, (2011).
14. F. Pfeiffer, T. Weitkamp, O. Bunk, and C. David. "hase retrieval and differential phase-contrast imaging with low-brilliance X-ray sources. *Nat. Phys.*, (2006).
15. T. E. Gureyev, S. C. Mayo, D. E. Myers, Ya. Nesterets, D. M. Paganin, A. Pogany, A. W. Stevenson, and S. W. Wilkins. efracting Rontgen' rays: propagation-based X-ray phase contrast for biomedical imaging. *J. Appl. Phys.*, (2009).
16. X. Wu and H. Liu. "A new theory of phase-contrast X-ray imaging based on Wigner distributions". *Med. Phys.*, (2004).
17. Pietro Ferraro, Sergio De Nicola, Andrea Finizio, Giuseppe Coppola, Simonetta Grilli, Carlo Magro, and Giovanni Pierattini. Compensation of the inherent wave front curvature in digital holographic coherent microscopy for quantitative phase-contrast imaging, *APPLIED OPTICS.*, (2003).
18. Alexander Chernobelsky, Oleg Shubayev Cindy R. Comeau, and Steven D. Wolff. Baseline Correction of Phase Contrast Images Improves Quantification of Blood Flow in the Great Vessels. *Journal of Cardiovascular Magnetic Resonance.*, (2007).
19. R A Lewis, N Yagi, M J Kitchen, M J Morgan, D Paganin, KKWSiu, K Pavlov, I Williams, K Uesugi, M J Wallace, C J Hall, JWhitley and S B Hooper. Dynamic imaging of the lungs using x-ray phase contrast. *Phys. Med. Biol.*, (2005).
20. Chulmin Joo, Taner Akkin, Barry Cense, Boris H. Park, and Johannes F. de Boer. Spectral-domain optical coherence phase microscopy for quantitative phase-contrast imaging. *OPTICS LETTERS.*, (2005).